Title:
Collateral development and arteriogenesis in hindlimbs of domestic swine after ligation of arterial inflow

Author List:
Patel NS[#1,2], Gao Y[#1], Aravind S[#1,2], Fuglestad M[1], Casale GP[1], *Pipinos II[##1,2], *Carlson MA[##1,2,3]

1. Department of Surgery, University of Nebraska Medical Center, Omaha, Nebraska
2. Surgery Department, Nebraska-Western Iowa Health Care System, Omaha, NE
3. Department of Genetics, Cell Biology and Anatomy, University of Nebraska Medical Center, Omaha, Nebraska

#These authors contributed equally
##These authors contributed equally
*Corresponding authors

Emails:
Patel, Neesha S (Neesha.patel@unmc.edu); Gao, Yue (ryan.gao@unmc.edu); Aravind, Shruthi (shruthi.aravind@unmc.edu); Fuglestad, Matthew (matthew.fuglestad@unmc.edu); Casale, George (gpcasale@unmc.edu); Pipinos, Iraklis I (ipipinos@unmc.edu); Carlson, Mark A (macarlso@unmc.edu)

Keywords: swine, porcine, animal models, arteriogenesis, ischemia, angiography, peripheral artery disease

ABSTRACT

Introduction. The development of collateral vasculature is a key mechanism compensating for arterial occlusions in patients with peripheral artery disease (PAD). We aimed to examine the development of collateral pathways after ligation of native vessels in a porcine model of PAD.

Methods: Right hindlimb Ischemia was induced in domestic swine (N=11, male, kg) using two different versions of arterial ligation. Version 1 (N=6) consisted of ligation/division of the right external iliac, profunda femoral (RPFA) and superficial femoral arteries (RSFA). Version 2 (N=5) consisted of the ligation of Version 1 with additional ligation/division of the right internal iliac artery (RIIA). Development of collateral pathways was evaluated with standard angiography at baseline (prior to arterial ligation) and at termination (4-8 weeks later). Relative luminal diameter of the arteries supplying the ischemic right hindlimb were determined by 2D angiography, as percent of the size of the distal aortic diameter.

Results: The dominant collateral pathway that developed after version 1 ligation connected the RIIA to the RPFA and RSFA/popliteal artery. Mean luminal diameter (± standard error) of the RIIA at termination increased by 38% ($P<0.05$) compared to baseline. Two co-dominant collateral pathways developed in version: (i) from the common internal iliac trunk and left internal iliac artery to the reconstituted RIIA, which then supplied the RPFA and RSFA/popliteal arteries; and (ii) from left profunda artery to the reconstituted RPFA. Mean diameter of the common internal iliac trunk and left profunda artery both increased at termination in the range of 20% ($p < 0.05$).

Conclusion: Two versions of hindlimb ischemia induction (right ilio-femoral artery ligation with and without right internal iliac artery ligation in swine produced differing collateral pathways,

along with changes to the diameter of the inflow vessels (i.e., arteriogenesis). Radiographic and anatomical data of the collateral formation in this porcine model should have value in investigation of the pathophysiology of hindlimb ischemia, and assessment of angiogenic therapies as potential treatments for PAD.

Abbreviations

ABI – Ankle/Brachial Index
CLI – Chronic Limb Ischemia
CIIT – Common Internal Iliac Trunk
LEIA – Left External Iliac Artery
LIIA – Left Internal Iliac Artery
LPFA – Left Profunda Femoral Artery
REIA – Right External Iliac Artery
RIIA – Right Internal Iliac Artery
RSFA – Right Superficial Femoral Artery
RPop – Right Popliteal Artery
PAD – Peripheral Arterial Disease
Moxy – Muscle Oximetry
SmO_2 – Muscle oxygen saturation
THb – Total Hemoglobin
dRPFA = reconstituted distal right profunda femoral artery;
dRIIA = reconstituted distal right internal iliac artery.

INTRODUCTION:

Peripheral artery disease (PAD) has a prevalence of 3- to 10%increasing to 15 to 20% in persons over 70 years [*1-3*] with an impact on functional status, quality of life, and life expectancy [*1-3*]. The vast majority of symptomatic PAD patients present with variations of exercise-associated leg discomfort and ambulatory disability known as intermittent claudication [*1-3*] while 1-2% present with a threatened ischemic limb. Treatment options for claudicating PAD patients include open and percutaneous revascularization; unfortunately of the PAD patients refered to vascular practicioners only 13% of patients with claudication and 50% of patients with critical limb ischemia end up receiving revascularization operations secondary to complex occlusive disease and medical comorbidities that limit the walking ability and/or increase the operative risk. For the rest of these patients, development of collateral blood flow is an important compensatory mechanism to improve blood flow to the ischemic limb, which makes the study of blood vessel growth in response to ischemia an important field of investigation.

The groups of Drs. Brewster and Lefer [*4,5*], in collaboration with our group, have demonstrated that multiple swine strains (with and without comorbidities) can recapitulate the pathophysiology of human PAD, including (i) persistently decreased hindlimb hemodynamics/perfusion, (ii) decreased treadmill performance, (iii) and ischemic myopathy (end-organ damage). The parallel between humans and swine prompted us to use a porcine model of PAD to determine 1) the pathways and size of the collaterals developing over thirty days after two different versions of ligation of native arteries supplying the hindlimb. 2) the effect of the ligation and of collateral development on limb hemodynamics and oxygenation. The rationale for studying this collateralization phenomenon was to develop a clinically-relevant large-animal platform in which the efficacy of cell-based therapies (or other interventions) in improving perfusion of the ischemic limb could be tested.

MATERIALS AND METHODS

Animal Welfare Statement. The animals utilized to generate the data for this report were maintained and treated in accordance with the *Guide for the Care and Use of Laboratory Animals* (8th ed.) from the National Research Council and the National Institutes of Health [*6*] and also in accordance with the Animal Welfare Act of the United States (U.S. Code 7, Sections 2131 – 2159). The animal protocol pertaining to this manuscript was approved by the Institutional Animal Care and Use Committee (IACUC) of the VA Nebraska-Western Iowa Health Care System (ID number 00950) and by the IACUC of the University of Nebraska Medical Center (ID number 15-068-07-ET). All procedures were performed in animal facilities approved by the Association for Assessment and Accreditation of Laboratory Animal Care International (AAALAC; www.aaalac.org) and by the Office of Laboratory Animal Welfare of the Public Health Service (grants.nih.gov/grants/olaw/olaw.htm). All surgical procedures were performed under isoflurane anesthesia, and all efforts were made to minimize suffering. Euthanasia was performed in accordance with the AVMA Guidelines for the Euthanasia of Animals [*7*].

Experimental Subjects. Wild type domestic swine (N = 13; castrated males; age 11-13 wk) were purchased from the Animal Research and Development Center at the University of Nebraska Lincoln (ardc.unl.edu). Swine were housed individually in pens, with multiple subjects per room, and fed ad lib with standard hog feed (Purina Nature's Match Sow and Pig Complete Feed).

Experimental Design. Refer to Fig. tf01. The basic experimental design included an ischemia-induction procedure (i.e., arterial ligation) on day 0, with endpoint measurement and necropsy

30 d later. Two methods of arterial ligation were compared in two nonrandomized groups of domestic swine; the groups were matched for age, size, and sex.

Set-Up and Anesthesia [*8*]. Swine were fasted for 24 h prior to the procedure, with free access to water and up to two 500cc bottles of regular Gatorade™. On day of procedure, each subject underwent induction with ketamine (Zoetis, 2.2 mg/kg), Telazol® (Zoetis; 4.4 mg/kg) and xylazine (Zoetis; 2.2 mg/kg), given combined in single IM injection. Each subject then was weighed and endotracheally intubated. EKG, pulse oximetry, rectal temperature, and lingual endtidal CO_2 ($EtCO_2$) monitors were placed. The subject was placed on a water-circulated warming blanket that was set at 102˚F. An auricular intravenous (IV) line was placed. Anesthesia was maintained with isoflurane (0.5-1%) and supplemental oxygen (3-5 L/min) using a Matrx® ventilator (midmark.com). The ventilator rate initially was set at 12-15 breaths per minute with a tidal volume of 10 mL/kg, and subsequently adjusted to maintain the EtCO2 at 40-50 mm Hg. Cotton blankets were placed over non-surgical areas to minimize loss of core temperature. Vital signs were continuously recorded to a laptop computer via a Bionet BM5 monitor (www.bionetus.com). A single dose of cefovecin sodium (Zoetis; 8 mg/kg IM) was given before incision.

Muscle Oximetry & Arterial Indices. Extremity muscle oximetry measurements were measured transcutaneously in the supine position under general anesthesia using an ANT Fortiori Design device (moxymonitor.com) with Peripedal software (peripedal.com); see Figs. tf11S and tf12S. The Moxy device has a noninvasive probe which measures muscle hemoglobin/myoglobin oxygen saturation (StO_2). For determination of arterial indices, a pediatric-size sphygmomanometer cuff was applied to each extremity (see Fig. tf11S), and systolic pressure was measured with the aid of doppler device [Model 811-B, Parks Medical Doppler (parksmed.com). The hindlimb arterial pressure index ("ABI", meant to be the porcine

analog of the clinical ankle-brachial index) was defined as the ratio of hindlimb systolic blood pressure over the higher of the two forelimb systolic pressure.

Laparotomy, Vessel Exposure, and Angiography. With the subject under general anesthesia and in the supine position, the chest, abdomen, groins, and bilateral lower extremities were shaved with an electric clipper, washed with soap and water, and then prepped using ChloraPrep™ applicators (chlorhexidine gluconate/isopropyl alcohol; BD Medical). In the first subject, vessel exposure was performed transabdominally through a right paramedian incision (Fig. tf10S), which began in the midline 7-8 cm above the urethral meatus and extended caudally to the right of the meatus and midline urethra and medial to the right-sided nipple line. Once in the peritoneal cavity, the viscera were gathered in a wet towel and retracted superiorly and to the left. The peritoneum overlying the distal aorta and trifurcation was incised, and the right hindlimb arterial system was exposed with sharp dissection. To gain access to the more distal right-sided pelvic vessels, the paramedian skin incision was extended over the right inguinal ligament and onto the right medial thigh, towards but not reaching the right stifle (knee) joint. The right inguinal ligament itself was not divided. For the subsequent ten subjects, vessel exposure was obtained with a retroperitoneal approach through a similar right paramedian incision that began level with the urethral meatus and medial to the right nipple line, and then extended inferiorly across the right inguinal ligament (not divided) and onto the right inner thigh. The abdominal wall layers were incised carefully down to the peritoneum, and then the dissection was performed laterally between the peritoneum and abdominal wall to develop the retroperitoneal space. The peritoneal sac, containing the intraabdominal organs, was retracted superiorly and to the left, which exposed the distal aorta and right-sided pelvic vasculature.
In all subjects an arterial line (20-gauge angiocatheter) was placed in the infrarenal aorta, 4-5 cm above the aortic trifurcation (refer to postmortem dissection in Fig. tf09S), through a site controlled with a 6-0 polypropylene U-stitch. This line was used for arterial blood pressure

monitoring and angiography. A baseline aortogram with runoff was obtained with injection of 10 mL of Visipaque™ 320 (Iodixanol; GE Healthcare) and C-arm fluoroscopy (GE OEC 9900 Elite).

Arterial Interruption. Once baseline angiography was obtained, the region of the aortic trifurcation was dissected. In the pig, the distal aorta trifurcates into the right and left external iliac arteries (REIA and LEIA) and the common internal iliac trunk (CIIT); the latter then bifurcates into the right and left internal iliac arteries (RIIA and LIIA; see Figs. tf09S and tf02A). The REIA then was dissected down to the bifurcation of the right superficial femoral artery (RSFA) and profunda femoris artery (RPFA). The REIA, right lateral circumflex iliac and lateral circumflex femoral artery (RLCIA and RLCFA, respectively) then were suture ligated proximally with 3-0 Silk (Figs. tf02B and tf03). Distal dissection exposed the bifurcation of the RSFA into the right popliteal and saphena arteries (RPop and RSA, respectively; Fig tf02A). The RSFA was suture ligated distal to the takeoff of the RLCFA (Figs. tf02B and tf03). A continuous segment of the REIA-RSFA was then excised (Figs. tf02B and tf03). This series of steps constituted the version 1 arterial interruption procedure. Version 2 (Figs. tf02C and tf05) consisted of version 1 plus ligation of the RIIA. To summarize:

Version 1 Interruption (Fig tf02B): ligation of the REIA, RSFA, RPFA, RLCIA, RLCFA and excision of a continuous segment of the REIA-RSFA.

Version 2 Interruption (Fig. tf02C): version 1 + RIIA ligation

A completion angiogram was performed after each arterial interruption procedure. The aortic puncture site utilized for angiographic access then was closed by tying the previously-placed U-stitch. The abdominal incision was closed anatomically in layers, with 2-0 polyglactin 910 in the peritoneum and posterior layers, 0-polydioxanone in the anterior aponeurosis, 3-0 polyglactin

910 in the panniculus carnosus, and 4-0 polyglactin 910 in the skin. Cyanoacrylate glue was applied over the skin incision; no other incisional dressing was applied. The animal's recovery from anesthesia was monitored until the subject was awake and mobile. Subjects were given half of their typical feed intake on post-ligation day 1, and were placed back on ad lib feeds on day 2.

Terminal procedure: Subjects underwent their terminal procedure 4 weeks after arterial interruption. After induction of general endotracheal anesthesia, the right carotid artery was exposed with a cervical cut-down. Hindlimb perfusion measurements (muscle oximetry and arterial indices) were performed as described above. A catheter was then placed into the right common carotid artery and advanced into the aorta using the Seldinger technique. An abdominal aortogram with distal runoff was performed. Bilateral hindlimb dissection was performed prior to euthanasia, and biopsies of the medial heads of the bilateral gastrocnemius were obtained (Fig. tf13S) and were processed as described below in section "Bright-Field Microscopy".

Arterial Diameter Analysis: Each angiogram obtained during the procedure was saved into the Digital Imaging and Communications in Medicine (DICOM) format within the GE OEC 9900 Elite C-arm. Images subsequently were accessed and analyzed using the RadiANT DICOM Viewer (Version 4.0.2). The cross-sectional diameter of the distal aorta was defined as 10 units. Relative diameter of each distal artery was then expressed in units of distal aortic diameter.

Bright-Field Microscopy: Samples from the medial gastrocnemius muscle were taken from the ischemic right hindlimbs and the contralateral non-ischemic hindlimbs of the swine at the end of the terminal procedure. Additionally, gastrocnemius muscle samples from a claudicating PAD patient and a control subject were harvested, in accordance with a protocol approved by the

Internal Review Board of the VA Nebraska Medical Center. The samples were obtained from the anteromedial aspect of the muscle belly 10 cm distal to the tibial tuberosity. Muscle specimens were fixed immediately into cold methacarn. After 48 hours in methacarn, the specimens were transferred to cold ethanol:H_2O (50:50v/v) and subsequently embedded in paraffin, sectioned at 4 microns, and mounted to glass slides. Slide specimens were deparaffinized in xylene and rehydrated to water. Images of specimens stained with hematoxylin and eosin were captured under bright-field illumination with a Leica DMRXA2 microscope (North Central Instruments), configured with a Leica DFC color camera (North Central Instruments).

Statistical analysis: Data were analyzed using ANOVA within Microsoft Excel; the level of significance was defined as $p < 0.05$.

RESULTS

Perioperative Events. Mean subject starting weight was 32.8 ± SD 4.0 kg (range = 26.6 – 39.0 kg, N = 6) and 37.0 ± 10.5 kg (range = 35.0 – 55.6 kg, N = 5) for versions 1 and 2, respectively; starting weight was not different between groups ($p = 0.19$, unpaired t-test). A total of 13 subjects underwent the ligation procedure. One pig developed rectal prolapse four days after operation and was euthanized; another pig expired on postoperative day one secondary to intestinal ischemia. Necropsy of the latter subject revealed a stomach distended with feed, but otherwise was inconclusive; all mesenteric vessels were patent. Of the eleven subjects which survived to the scheduled termination (N = 6 for version 1 and N = 5 for version 2), two subjects (one of each version) developed clinically-apparent ischemia of the right hoof, manifested by ulcer formation on the weight-bearing region. Their mobility was affected, but each animal could still ambulate and both survived until scheduled termination.

Arterial Pressure Indices at rest. One subject's ABI data (version 1) were missing, so ten subjects underwent analysis of resting ABI data. The ABI was calculated pre-ligation and immediately post-ligation on day 0, and then at pre-necropsy on day 30; see Table 1. The mean ABI was not different at rest between the two ligation versions at any individual time point, including at pre-necropsy. Immediately post-ligation, the ABI dropped to zero for both versions. At 30 d (pre-necropsy), the mean ABI had recovered in both groups to ~0.6.

Muscle hemoglobin/myoglobin oxygen saturation (StO_2) at rest. StO_2 measurements were not different at rest between the two ligation versions at any single time point, including pre-necropsy (Fig. tf07). The StO_2 value decreased from 60-70% pre-ligation to ~20% immediately post-ligation in both versions in the affected limb, with recovery to ~40% at 30 d (pre-necropsy).

Interestingly, the contralateral (left, untreated) hindlimb demonstrated a parallel though less profound effect on StO_2 readings, again with partial recovery at 30 d (Fig. tf07).

Collateral Pathway Development. Refer to Videos 1-12 in the Supplemental Material. Sample images (video stills) of the pre-ligation (baseline) aortogram with runoff angiography for versions 1 and 2 are shown in Figs. tf04A and tf06A, respectively (see accompanying Videos 1-2 and 7-8, respectively). Immediately after ligation in version 1, the REIA-RSFA segment is no longer present and there is delayed filling of the RFPA and remaining distal arteries from the patent and unligated RIIA, with some lesser contribution through circumflex collaterals (Fig. tf04B and Videos 3-4). After 30 days of ischemia in version 1, pre-necropsy angiography (Fig. tf04C) demonstrated that the RIIA was noticeably enlarged, and that collateral vessels from the RIIA quickly reconstituted the RPFA, followed by the RFSFA/RPop reconstitution (Video 5-6). There also appeared to be some minor contribution to this RPFA/RSFA/RPop reconstitution through lumbar/circumflex vessels. Immediately after ligation in version 2, both the REIA and RIIA are no longer present and there is delayed filling of the RPFA from the LPFA (through cross-pelvic collaterals) shown in Fig. tf06B and Videos 9-10. In addition, there may have been some collateral supply to the ischemic hindlimb through the right lumbar vessels immediately after ligation in version 2 (Videos 9-10). After 30 days of ischemia in version 2, pre-necropsy angiography (Fig. tf06C) demonstrated the presence of two co-dominant collateral pathways that supplied the ischemic right hindlimb. The first pathway connected the CIIT and LIIA to the reconstituted RIIA, which then supplied the RPFA and RSFA/RPop (Videos 11-12). The second pathway connected the LPFA to the reconstituted RPFA (i.e., the same pathway noted immediately after ligation).

Arteriogenesis. The relative arterial diameters of the hindlimb arteries at pre-ligation (day 0) and pre-necropsy (day 30) are shown in Table 2. At baseline (i.e., day 0), the mean diameter of

the LEIA and the dRPFA (dRPFA = reconstituted distal right profunda femoral artery); were 6% and 30% larger, respectively, in the version 2 compared to the version 1 subjects ($p < 0.05$). After 30 days of ischemia in version 1 subjects, the CIIT, RIIA, and dRPFA increased in diameter by 17%, 38%, and 17%, respectively ($p < 0.05$); the LIIA and RPop both trended toward increased diameter, but did not reach significance. The dRPFA and RPop both represented reconstituted vessels at 30 days, as described above. After 30 days of ischemia in version 2 subjects, the CIIT, LEIA, LIIA, and LPFA all had a diameter increase in the range of 20% (23%, 18%, 21%, and 26%, respectively); the dRPFA trended toward increased diameter, but did not reach significance. The only vessel noted to have a decrease in mean diameter at 30 days was the RPop in the version 2 subjects, which decreased by 21%.

Chronically Ischemic Muscle of Porcine and Human Origin Exhibits Myopathic Features, As Determined by Bright-Field Microscopy: Refer to Fig. tf08. Histological changes in gastrocnemius muscle from chronically ligated hindlimbs (Fig. tf08D) were determined in reference to the contralateral control hindlimbs (Fig. tf08B) and compared with ischemic (Fig. tf08C) and control (Fig. tf08A) muscle from claudicating PAD and control non-PAD patients, respectively. Control muscle from swine (Fig. tf08B) and human (Fig. tf08A) gastrocnemius demonstrated polygonal myofibers of similar shape and size with barely perceptible extracellular matrix around myofibers (endomysium) and myofscicles (perimysium). In the ischemic hindlimb of the swine (Fig. tf08D), we found myofiber degeneration and fibrosis that were very similar to that of the claudicating PAD patient (Fig. tf08C) exhibited a wider range of myofiber size from irregularly shaped microfibers along with endomysial and perimysial fibrosis.

DISCUSSION

The findings presented here establish the pattern and relative size of the collateral pathways developing after ligation of native vessels in a porcine model of PAD. Our data demonstrate that two versions of hindlimb ischemia induction (right ilio-femoral artery ligation with and without right internal iliac artery ligation) produce differing collateral pathways along with outward remodeling/arteriogenesis (seen as increases of the diameter) of the major inflow vessels. We found that after ligation and excision of the right iliofemoral artery a dominant pathway develops connecting the RIIA to the RPFA and RSFA/popliteal artery of the ischemic limb. Furthermore, after ligation and excision of the right iliofemoral artery with concomitant ligation/division of the RIIA two co-dominant collateral pathways develop to perfuse the right hindlimb. The first pathway connects the common internal iliac trunk and left internal iliac artery to the reconstituted RIIA which then supplies the RPFA and RSFA/popliteal arteries. The second pathway connects the left profunda artery to the reconstituted RPFA. Furthermore, our data confirm the findings of the groups of Drs. Brewster and Lefer and demonstrate the ability of all strains of swine tested thus far (with and without comorbidities, Ossabaw mini swine, Yorkshire swine fed regular chow and domestic swine fed regular chow), undergoing endovascular or open arterial occlusions, to recapitulate the pathophysiologic characteristics of human PAD, including decreased hindlimb hemodynamics/perfusion, and ischemic myopathy (end-organ damage). In particular the ischemic myopathy has been virtually identical to that found in patients.

The development of collateral vasculature is a key mechanism compensating for arterial occlusions and may be manipulated therapeutically to treat patients with Peripheral Artery Disease (PAD). In previous published work our group and others have found the swine to be a clinically-relevant large animal model of PAD, because of its similarities with the human patient with respect to size, anatomy, physiology, comorbidities, and suitability for invasive/non-invasive

testing and treatment [*4,5*]. In this work we continue to characterize the swine model of hindlimb ischemia focusing on the description of its baseline, innate ability to develop collaterals around two patterns of iatrogenic occlusions of the arterial supply to the hindlimb. We believe that this work can serve as a reference for future studies of the efficacy of therapeutic interventions on collateral growth. In particular, the advent of different angiogenic therapies for humans [*9-11*] including administration of angiogenic cytokines, either as recombinant protein or as gene therapy, and more recently, to investigations of stem/progenitor cell therapy has opened a new frontier in therapeutic medicine. This porcine animal model can help in the evaluation and optimization of these modalities and in the exploration of questions such as the optimal dosing and delivery method for angiogenic therapy [*10,12-15*].

In prior work the groups of Drs. Brewster and Lefer in collaboration with our team have used Ossabaw swine with metabolic syndrome and Yorkshire swine fed regular chow and an innovative endovascular approach (using stent grafts and endovascular occluders) to produce right hindlimb ischemia. In the current work we used the domestic swine fed regular diet and an open approach to the introduction of arterial ligations. This approach allows for relative cost saving (less expensive animal, lower cost of operative and device supplies and lower cost of diet) and can be done by a team with open surgical skills without the need for endovascular skill or operative setup needed, while maintaining the ability to tailor the degree of ischemia required (changing the number and pattern of arteries being ligated). The main limitation of this model in comparison to the endovascular occlusion is the requirement of large incisions for the performance of the arterial ligation procedure. The degree of tissue manipulation and pain associated with this procedure could potentially present as a cofounding factor when studying potential aspects such as functional status and gait of the subjects. It is possible that stress of this relatively involved open operation was the main reason behind the two major complications in our group of animals. The rectal prolapse is common in growing swine from 8 to 20 weeks old and in our case it was likely produced by an increase in intra-abdominal pressure from

postoperative ileus. In the swine with intestinal ischemia the necropsy revealed a stomach distended with recent feed while all mesenteric vessels were patent. Apparently the directions for preoperative fast were not observed and the subject had eaten a large amount of food the day prior to the operation. In response to this event we corrected the problem in the communication with the animal care personnel and have been able to strictly observe the preoperative diet preparation. When a 24 hour fast prior to the procedure, with free access to water and up to two 500cc bottles of regular Gatorade™ is observed, no additional intraabdominal complications occurred. Two of the eleven subjects which survived to the scheduled termination (one of each version) developed ulcers of their hoof on the weight-bearing region. This demonstrates that our approach to hindlimb ischemia produces a model of severe claudication and in some cases critical limb ischemia.

Another aspect that is unique to this project is the careful characterization of arteriogenesis and collateral formation. We were able to demonstrate the specific locations within the porcine vascular network that experienced the greatest growth after induction of ischemia. The quantification of the specific arterial growth was used to support the subjective finding of the reproducible collateral formation we observed amongst the different versions of hindlimb ischemia. It is believed that arteriogenesis is a reactive process to the blood flow redistribution that occurs in occlusive disease [*16-19*]. The changes in fluid dynamics of the downstream vessels causes an increase in shear forces that leads to upregulation of the cell adhesion molecules with subsequent rise in cytokines and growth factors, and ultimately to the endothelial and smooth cell proliferation that results when the arterial lumen increases. Given the current understanding of the pathophysiology of the vessel remodeling that occurs in PAD, we can use the swine ischemia model to test angiogenic therapies in a quantitative fashion, as well as investigating/improving delivery method, dosing targets, and the effectiveness of various therapies.

The work we present has several limitations. First is the acute nature of the onset of

ischemia in the model which differs from the more progressive and chronic nature of human PAD. Furthermore patients with PAD often have significant comorbidities such as hypertension, dyslipidemia and diabetes. Our swine population did not have any of these comorbidities and it could impact the veracity of this model. Furthermore all of our measurements of hemodynamic (hindlimb over forelimb index) and perfusion changes (muscle hemoglobin/myoglobin oxygen saturation) were measured at rest and small but important changes may not be captured by resting measurements. Future work needs to increase the sophistication and complexity of the testing to include measurements during stress (either post-occlusive hyperemia or exercise-induced). Finally, our work focused on measurements of arteriogenesis in the larger inflow arteries. It is likely that similar changes are present in smaller, unnamed collateral arteries and these should be evaluated in future works.

CONCLUSION

Our open swine hindlimb ischemia model holds great promise in the translational research of PAD. The deliberate characterization of the collateral network formation, and the objective measurement of the arteriogenesis that occurs are unique and pioneering. With a quantitated understanding of the vascular remodeling that develops with our ischemia model, we can utilize it to empirically test future therapies in our goal of optimizing existing treatment regimens or innovating novel therapies in the study of PAD.

REFERENCES

1. Benjamin EJ, Blaha MJ, Chiuve SE, Cushman M, Das SR, Deo R, et al. Heart Disease and Stroke Statistics-2017 Update: A Report From the American Heart Association. *Circulation* 2017; 135(10): e146-e603. PMID: 28122885. doi: 10.1161/CIR.0000000000000485.
2. Norgren L, Hiatt WR, Dormandy JA, Nehler MR, Harris KA, Fowkes FG. Inter-Society Consensus for the Management of Peripheral Arterial Disease (TASC II). *J Vasc Surg* 2007; 45 Suppl S: S5-67. PMID: 17223489. doi: 10.1016/j.jvs.2006.12.037.
3. Roger VL, Go AS, Lloyd-Jones DM, Benjamin EJ, Berry JD, Borden WB, et al. Executive summary: heart disease and stroke statistics--2012 update: a report from the American Heart Association. *Circulation* 2012; 125(1): 188-97. PMID: 22215894. doi: 10.1161/CIR.0b013e3182456d46.
4. Polhemus DJ, Bradley JM, Islam KN, Brewster LP, Calvert JW, Tao YX, et al. Therapeutic potential of sustained-release sodium nitrite for critical limb ischemia in the setting of metabolic syndrome. *Am J Physiol Heart Circ Physiol* 2015; 309(1): H82-92. PMID: 25910804. doi: 10.1152/ajpheart.00115.2015.
5. Long CA, Timmins LH, Koutakis P, Goodchild TT, Lefer DJ, Pipinos, II, et al. An endovascular model of ischemic myopathy from peripheral arterial disease. *J Vasc Surg* 2017; 66(3): 891-901. PMID: 27693032. doi: 10.1016/j.jvs.2016.07.127.
6. Committee for the Update of the Guide for the Care and Use of Laboratory Animals. *Guide for the Care and Use of Laboratory Animals*: Washington, DC: The National Academies Press; 2011.

7. American Veterinary Medical Association Panel on Euthanasia. *AVMA Guidelines for the Euthanasia of Animals: 2013 Edition*. Schaumberg, IL: American Veterinary Medical Association; 2013.

8. Swindle MM, Smith AC. *Swine in the Laboratory: Surgery, Anesthesia, Imaging, and Experimental Techniques*. 3rd ed. Boca Raton, FL: CRC Press; 2016.

9. Cooke JP, Losordo DW. Modulating the vascular response to limb ischemia: angiogenic and cell therapies. *Circ Res* 2015; 116(9): 1561-78. PMID: 25908729. doi: 10.1161/CIRCRESAHA.115.303565.

10. Frangogiannis NG. Cell therapy for peripheral artery disease. *Curr Opin Pharmacol* 2018; 39: 27-34. PMID: 29452987. doi: 10.1016/j.coph.2018.01.005.

11. Parikh PP, Liu ZJ, Velazquez OC. A Molecular and Clinical Review of Stem Cell Therapy in Critical Limb Ischemia. *Stem Cells Int* 2017; 2017: 3750829. PMID: 29358955. doi: 10.1155/2017/3750829.

12. Aranguren XL, Verfaillie CM, Luttun A. Emerging hurdles in stem cell therapy for peripheral vascular disease. *J Mol Med (Berl)* 2009; 87(1): 3-16. PMID: 18712330. doi: 10.1007/s00109-008-0394-3.

13. Gupta NK, Armstrong EJ, Parikh SA. The current state of stem cell therapy for peripheral artery disease. *Curr Cardiol Rep* 2014; 16(2): 447. PMID: 24414120. doi: 10.1007/s11886-013-0447-2.

14. Lawall H, Bramlage P, Amann B. Treatment of peripheral arterial disease using stem and progenitor cell therapy. *J Vasc Surg* 2011; 53(2): 445-53. PMID: 21030198. doi: 10.1016/j.jvs.2010.08.060.

15. Qadura M, Terenzi DC, Verma S, Al-Omran M, Hess DA. Concise Review: Cell Therapy for Critical Limb Ischemia: An Integrated Review of Preclinical and Clinical Studies. *Stem Cells* 2018; 36(2): 161-71. PMID: 29226477. doi: 10.1002/stem.2751.

16. Carmeliet P, Eelen G, Kalucka J. Arteriogenesis versus angiogenesis. In: Krams R, Bäck M, editors. The ESC Textbook of Vascular Biology: Oxford University Press; 2017.

17. Deindl E, Schaper W. The art of arteriogenesis. *Cell Biochem Biophys* 2005; 43(1): 1-15. PMID: 16043879. doi: 10.1385/CBB:43:1:001.

18. Rizzi A, Benagiano V, Ribatti D. Angiogenesis versus arteriogenesis. *Rom J Morphol Embryol* 2017; 58(1): 15-9. PMID: 28523292. doi:

19. van Royen N, Piek JJ, Schaper W, Fulton WF. A critical review of clinical arteriogenesis research. *J Am Coll Cardiol* 2009; 55(1): 17-25. PMID: 20117358. doi: 10.1016/j.jacc.2009.06.058.

ACKNOWLEDGEMENTS

This study is the result of work supported in part with resources and the use of facilities at the Omaha VA Medical Center (Nebraska-Western Iowa Health Care System). This work also was supported with internal seed funds provided by the University of Nebraska Medical Center Department of Surgery. Portions of this study were presented at Vascular Discovery: From Genes to Medicine (San Francisco, CA; May, 2018). The authors would like to acknowledge the technical assistance of Chris Hansen.

DISCLOSURES

The authors declare no competing interests.

FIGURE LEGENDS

Fig. tf01-tf08, contained within the Figure Legends.

SUPPLEMENTAL MATERIAL

Supplemental Fig. tf09S-tf13S.

Videos

1. “Vid01_v1_PreLigAngio_Proximal.mp4”. Description: Version 1 aortobifemoral angiography shot pre-ligation, proximal view.
2. “Vid02_v1_PreLigAngio_Distal.mp4”. Description: Version 1 aortobifemoral angiography shot pre-ligation, distal view.
3. “Vid03_v1_PostLigAngio_Proximal.mp4”. Description: Version 1 aortobifemoral angiography shot immediately post-ligation, proximal view.
4. “Vid04_v1_PostLigAngio_Distal.mp4”. Description: Version 1 aortobifemoral angiography shot immediately post-ligation, distal view.
5. “Vid05_v1_PreNecAngio_Proximal.mp4”. Description: Version 1 aortobifemoral angiography shot immediately pre-necropsy (30 days after ligation), proximal view.
6. “Vid06_v1_PreNecAngio_Distal.mp4”. Description: Version 1 aortobifemoral angiography shot immediately pre-necropsy (30 days after ligation), distal view.
7. “Vid07_v2_PreLigAngio_Proximal.mp4”. Description: Version 2 aortobifemoral angiography shot pre-ligation, proximal view.
8. “Vid08_v2_PreLigAngio_Distal.mp4”. Description: Version 2 aortobifemoral angiography shot pre-ligation, distal view.
9. “Vid09_v2_PostLigAngio_Proximal.mp4”. Description: Version 2 aortobifemoral angiography shot immediately post-ligation, proximal view.
10. “Vid10_v2_PostLigAngio_Distal.mp4”. Description: Version 2 aortobifemoral angiography shot immediately post-ligation, distal view.
11. “Vid11_v2_PreNecAngio_Proximal.mp4”. Description: Version 2 aortobifemoral angiography shot immediately pre-necropsy (30 days after ligation), proximal view.
12. “Vid12_v2_PreNecAngio_Distal.mp4”. Description: Version 2 aortobifemoral angiography shot immediately pre-necropsy (30 days after ligation), distal view.

Table 1. Arterial pressure indices ("ABI") of right (ischemic) hindlimb in Version 1 vs. 2.

	Day 0			
Version (N)	ABI, pre	ABI, post	ABI, Day 30	*ANOVA
1 (N = 5)	1.00 ± 0.22	0	0.62 ± 0.25	0.0001
2 (N = 5)	1.24 ± 0.30	0	0.62 ± 0.35	0.0004
*Unpaired t-test	0.196	1.000	0.968	

ABI expressed as mean ± standard deviation. Terms "pre" and "post" refer to before and after arterial ligation. The 30 d ABI was determined immediately prior to necropsy. *p-values.

Table 2. Relative hindlimb arterial diameters, Version 1 vs. 2, at days 0 vs. 30.

	CIIT		LEIA		RIIA		LIIA		dRPFA		LPFA		RPop	
VERSION 1	Day 0	Day 30	Day 0	Day 30	Day 0	Day 30	Day 0	Day 30	Day 0	†Day 30	Day 0	Day 30	Day 0	†Day 30
Mean	6.70	7.87	5.51	5.37	3.75	5.19	3.65	3.85	2.58	3.02	3.25	3.25	3.24	3.00
SD	0.34	0.44	0.27	0.26	0.31	0.22	0.19	0.24	0.29	0.25	0.25	0.39	0.37	0.32
*Paired t	**0.0049**		0.1901		**0.0001**		0.0702		**0.0228**		0.4936		0.0529	
	CIIT		LEIA		dRIIA		LIIA		dRPFA		LPFA		RPop	
VERSION 2	Day 0	Day 30	Day 0	Day 30	Day 0	†Day 30	Day 0	Day 30	Day 0	†Day 30	Day 0	Day 30	Day 0	†Day 30
Mean	6.68	8.24	5.84	6.92	3.13	3.44	3.90	4.72	3.35	3.67	3.50	4.42	3.37	2.65
SD	0.26	0.85	0.32	0.75	0.24	0.74	0.33	0.33	0.39	0.18	0.35	1.03	0.39	0.40
*Paired t	**0.0158**		**0.0133**		0.1304		**0.0044**		0.0591		**0.0207**		**0.0187**	
**Unpaired t	0.4678	0.1892	**0.0465**	**0.0005**	**NA**	**NA**	0.0727	**0.0004**	**0.0023**	**0.0004**	0.0917	**0.0145**	0.2892	0.0710

Relative diameter of each artery was expressed in units of distal aortic diameter (which was defined as 10 within each angiogram). Day 0 = pre-ligation measurement. Day 30 = pre-necropsy measurement. CIIT = common internal iliac trunk; LEIA = left external iliac artery; RIIA = right internal iliac artery; LIIA = left internal iliac artery; dRPFA = reconstituted distal right profunda femoral artery; LPFA = left profunda femoral artery; RPop = right popliteal artery; dRIIA = reconstituted distal right internal iliac artery. *Paired t-test compared day 0 vs. 30 for each artery (p-value). **Unpaired t-test compared Version 1 vs. Version 2 at each time point (p-value). †Reconstituted vessel. NA = comparison not applicable (RIIA was measured in Version 1, dRIIA was measured in Version 2).

Main figures

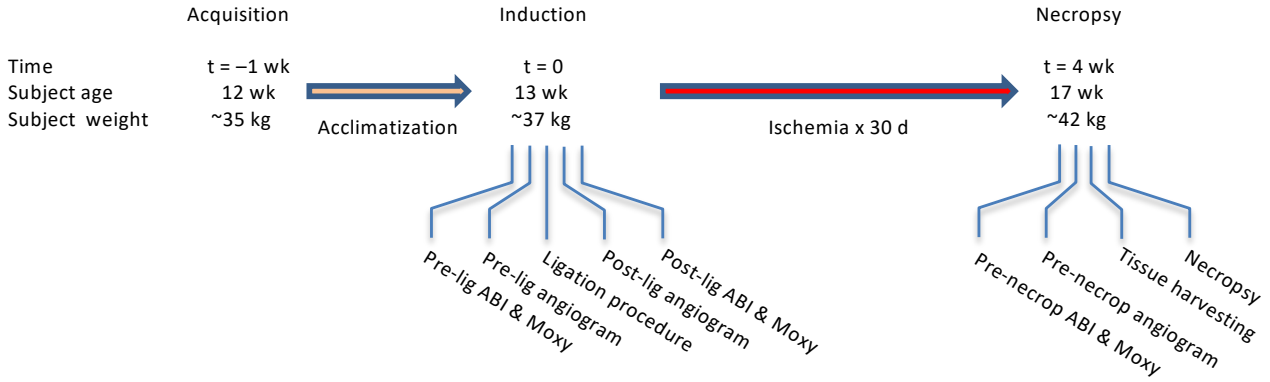

Fig. tf01. Experimental flow diagram. Domestic swine were 3 mo old at time of acquisition (t = -1 wk).

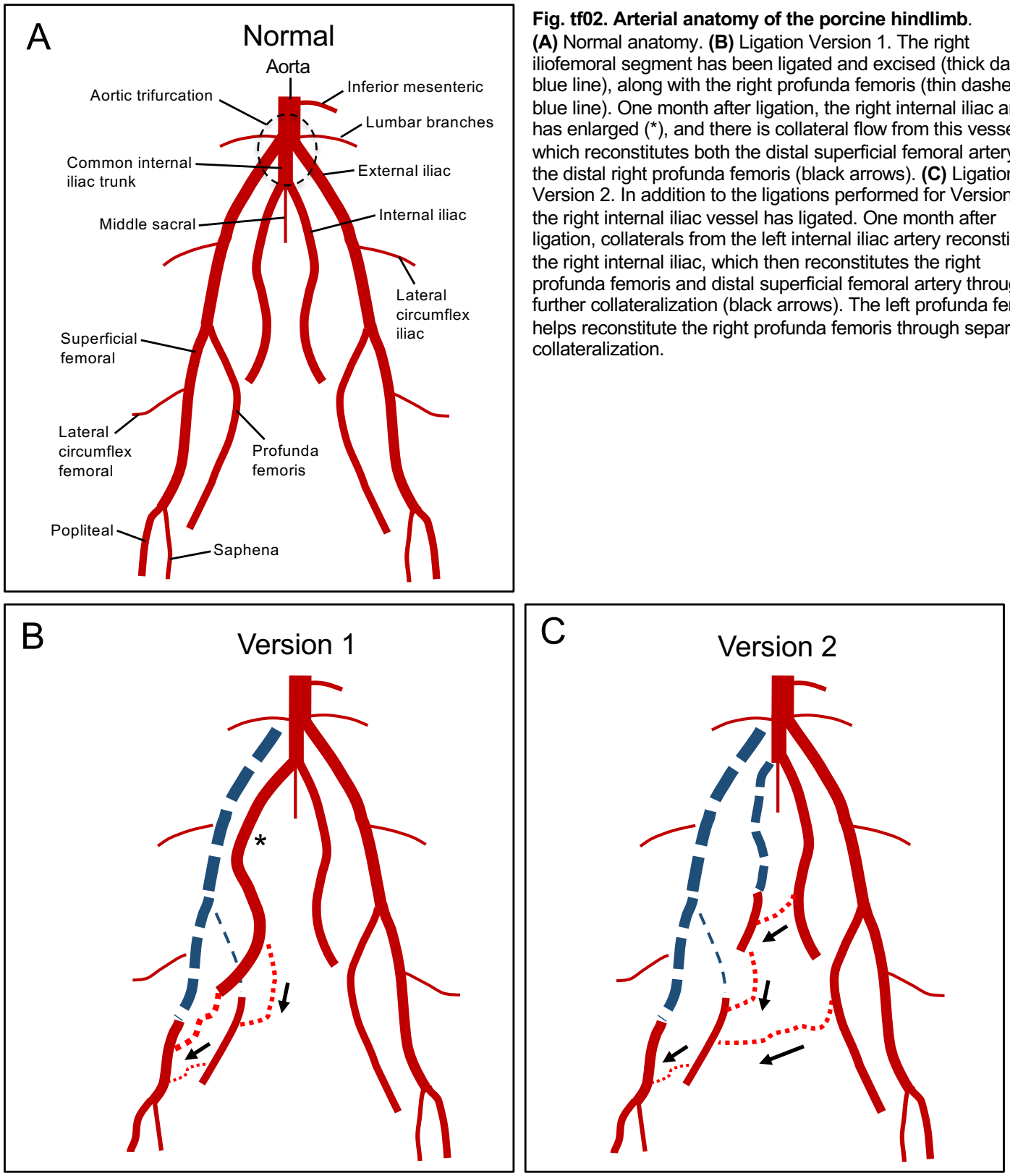

Fig. tf02. Arterial anatomy of the porcine hindlimb. **(A)** Normal anatomy. **(B)** Ligation Version 1. The right iliofemoral segment has been ligated and excised (thick dashed blue line), along with the right profunda femoris (thin dashed blue line). One month after ligation, the right internal iliac artery has enlarged (*), and there is collateral flow from this vessel which reconstitutes both the distal superficial femoral artery and the distal right profunda femoris (black arrows). **(C)** Ligation Version 2. In addition to the ligations performed for Version 1, the right internal iliac vessel has ligated. One month after ligation, collaterals from the left internal iliac artery reconstitute the right internal iliac, which then reconstitutes the right profunda femoris and distal superficial femoral artery through further collateralization (black arrows). The left profunda femoris helps reconstitute the right profunda femoris through separate collateralization.

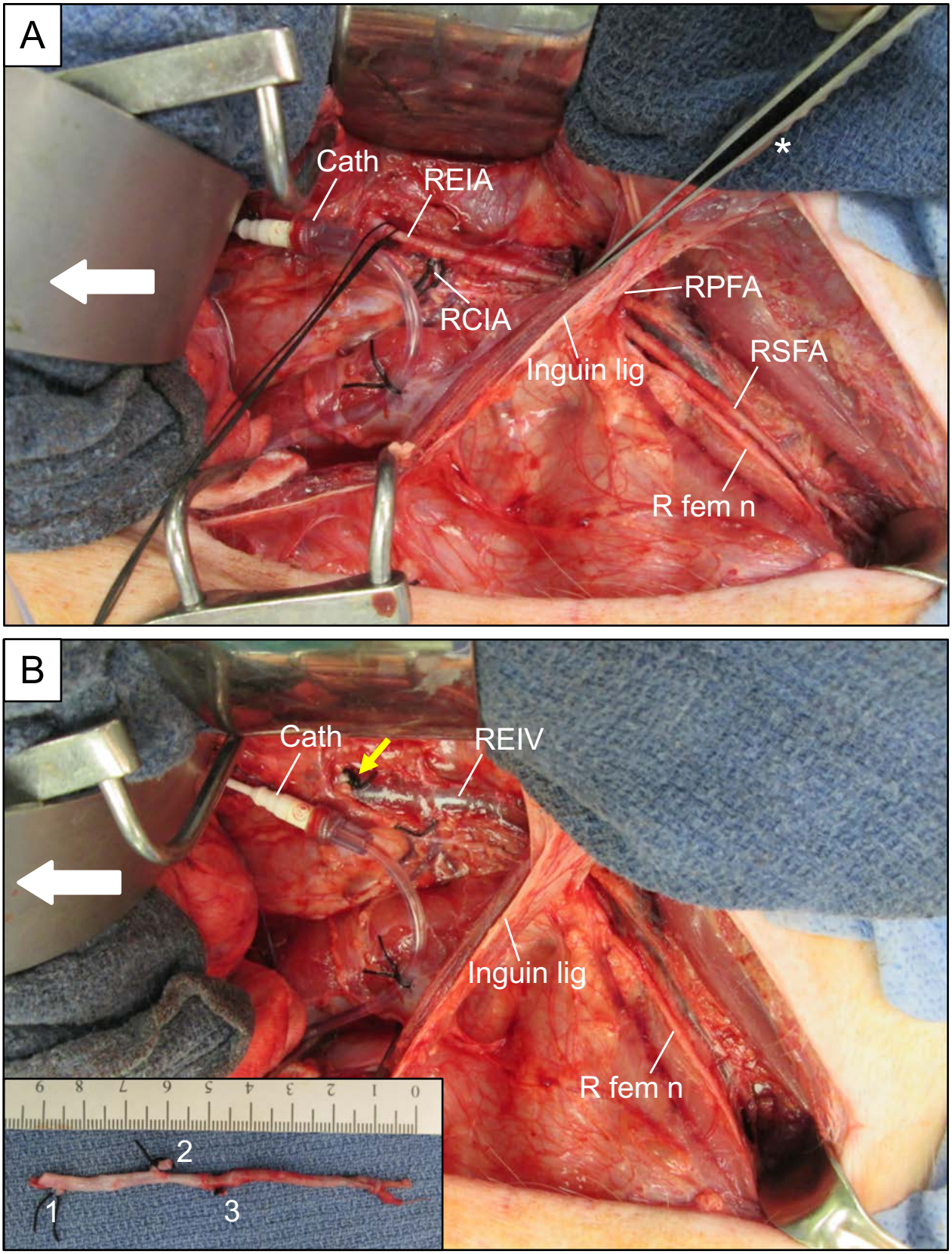

Fig. tf03. Ligation Version 1, intraoperative photos. **(A)** Prior to ligation, showing a right retroperitoneal dissection. Large white arrow is superior. The viscera have been retracted medially and superiorly. The right iliofemoral complex has been dissected out above and below the inguinal ligament. The REIA is shown with silk vessel loops placed proximally, in preparation for ligation. The RCIA already has been ligated with silk ties. The DeBakey forceps (*) is pushing the inguinal ligament inferiorly. **(B)** The right iliofemoral complex has been ligated and excised down to the distal RSFA, with ligation of the RPFA and RCIA. The right external iliac vein (REIV) is visible in the bed of the resected artery. The yellow arrow indicates the stump of the ligated REIA. **Inset**: resected segment of right iliofemoral vessel, with same orientation as main panel. 1 = stump of RCIA; 2 = stump of RPFA; 3 = stump of RCFA; scale = cm. Cath = Angiocatheter inserted into distal aorta, for angiography; Inguin lig = inguinal ligament; R fem n = right femoral nerve.

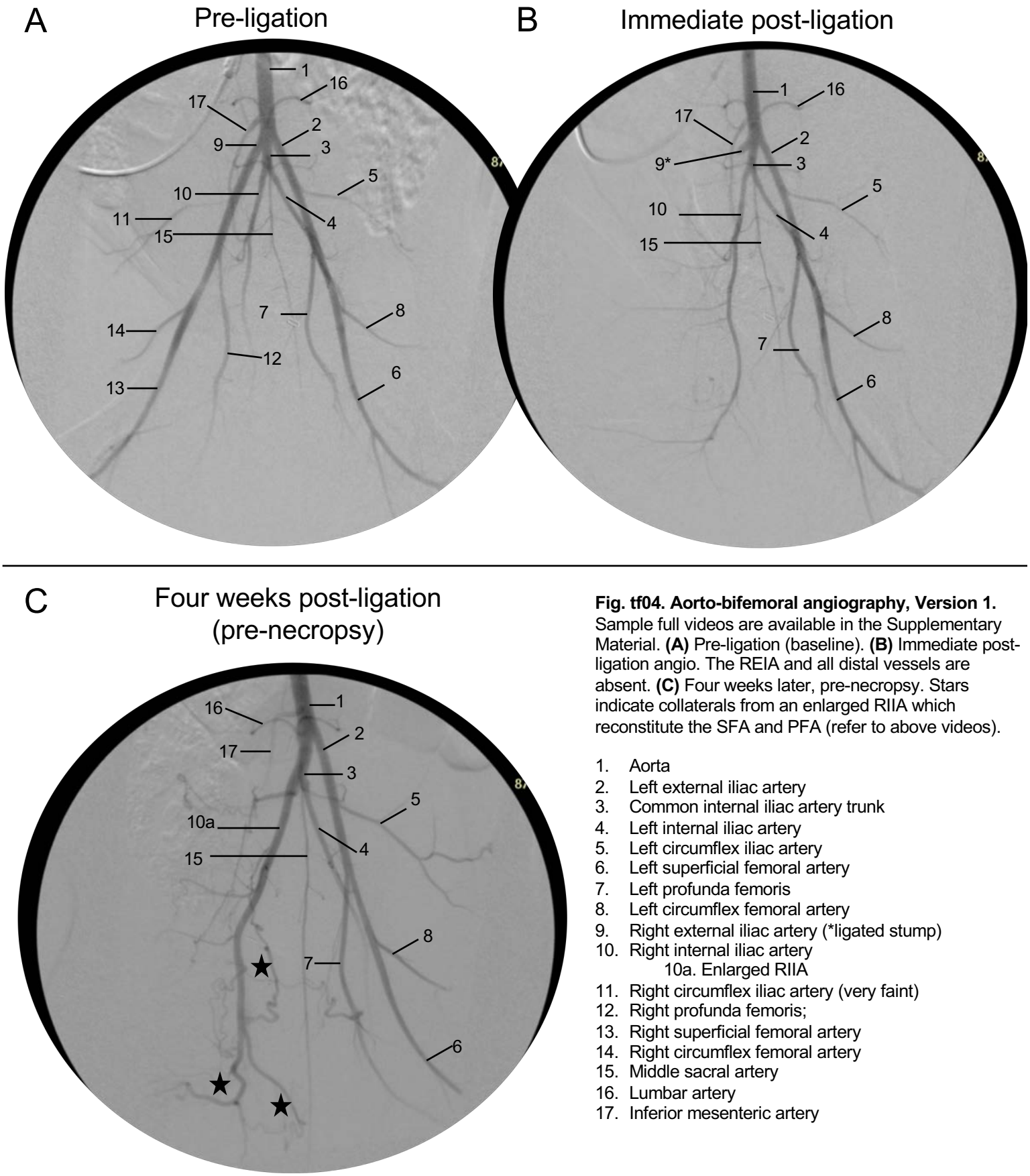

Fig. tf04. Aorto-bifemoral angiography, Version 1. Sample full videos are available in the Supplementary Material. **(A)** Pre-ligation (baseline). **(B)** Immediate post-ligation angio. The REIA and all distal vessels are absent. **(C)** Four weeks later, pre-necropsy. Stars indicate collaterals from an enlarged RIIA which reconstitute the SFA and PFA (refer to above videos).

1. Aorta
2. Left external iliac artery
3. Common internal iliac artery trunk
4. Left internal iliac artery
5. Left circumflex iliac artery
6. Left superficial femoral artery
7. Left profunda femoris
8. Left circumflex femoral artery
9. Right external iliac artery (*ligated stump)
10. Right internal iliac artery
    10a. Enlarged RIIA
11. Right circumflex iliac artery (very faint)
12. Right profunda femoris;
13. Right superficial femoral artery
14. Right circumflex femoral artery
15. Middle sacral artery
16. Lumbar artery
17. Inferior mesenteric artery

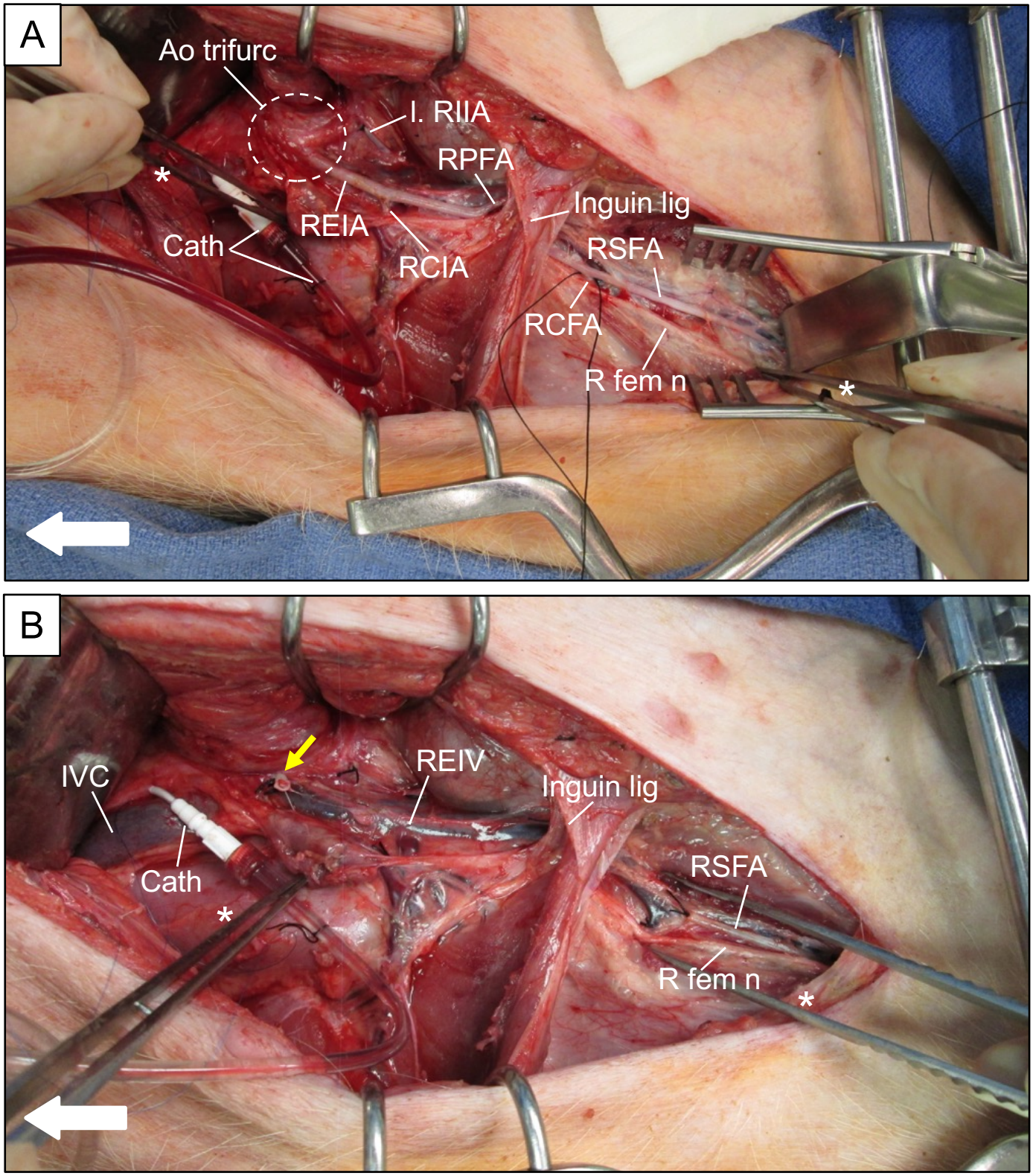

Fig. tf05. Ligation Version 2, intraoperative photos. **(A)** Prior to ligation, showing a right retroperitoneal dissection. Large white arrow is superior. The viscera have been retracted medially and superiorly. The right iliofemoral complex has been dissected out above and below the inguinal ligament. The region of the aortic trifurcation (Ao trifurc) is indicated with a dashed white circle. The RIIA already has been ligated. There is a silk loop around the RCFA. **(B)** The right iliofemoral complex has been ligated and excised down to the distal RSFA, with ligation of the RPFA and RCIA. The right external iliac vein (REIV) is visible in the bed of the resected artery. The yellow arrow indicates the stump of the ligated REIA. Labeling otherwise is similar to Fig. tf03.

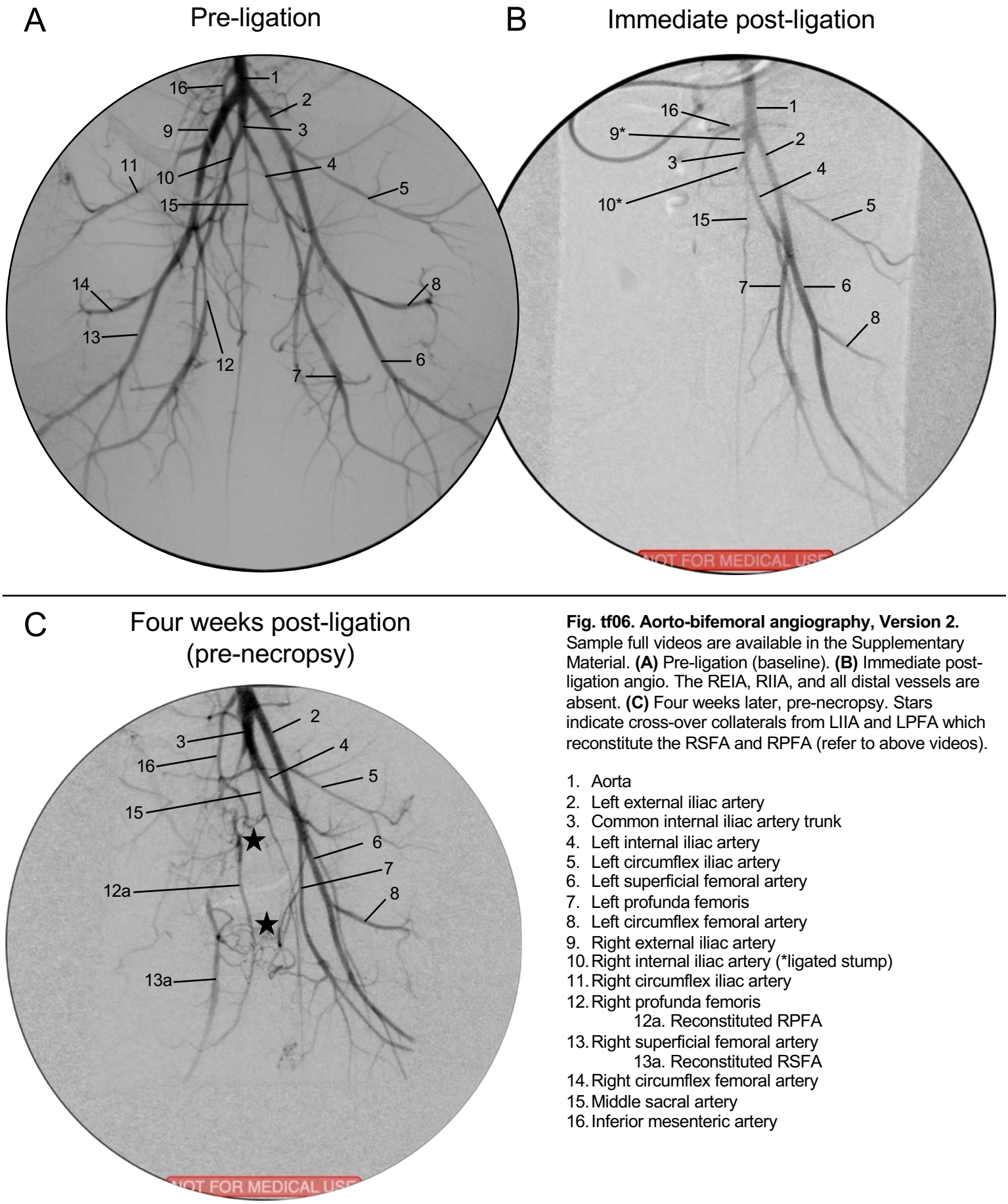

Fig. tf06. Aorto-bifemoral angiography, Version 2. Sample full videos are available in the Supplementary Material. **(A)** Pre-ligation (baseline). **(B)** Immediate post-ligation angio. The REIA, RIIA, and all distal vessels are absent. **(C)** Four weeks later, pre-necropsy. Stars indicate cross-over collaterals from LIIA and LPFA which reconstitute the RSFA and RPFA (refer to above videos).

1. Aorta
2. Left external iliac artery
3. Common internal iliac artery trunk
4. Left internal iliac artery
5. Left circumflex iliac artery
6. Left superficial femoral artery
7. Left profunda femoris
8. Left circumflex femoral artery
9. Right external iliac artery
10. Right internal iliac artery (*ligated stump)
11. Right circumflex iliac artery
12. Right profunda femoris
    - 12a. Reconstituted RPFA
13. Right superficial femoral artery
    - 13a. Reconstituted RSFA
14. Right circumflex femoral artery
15. Middle sacral artery
16. Inferior mesenteric artery

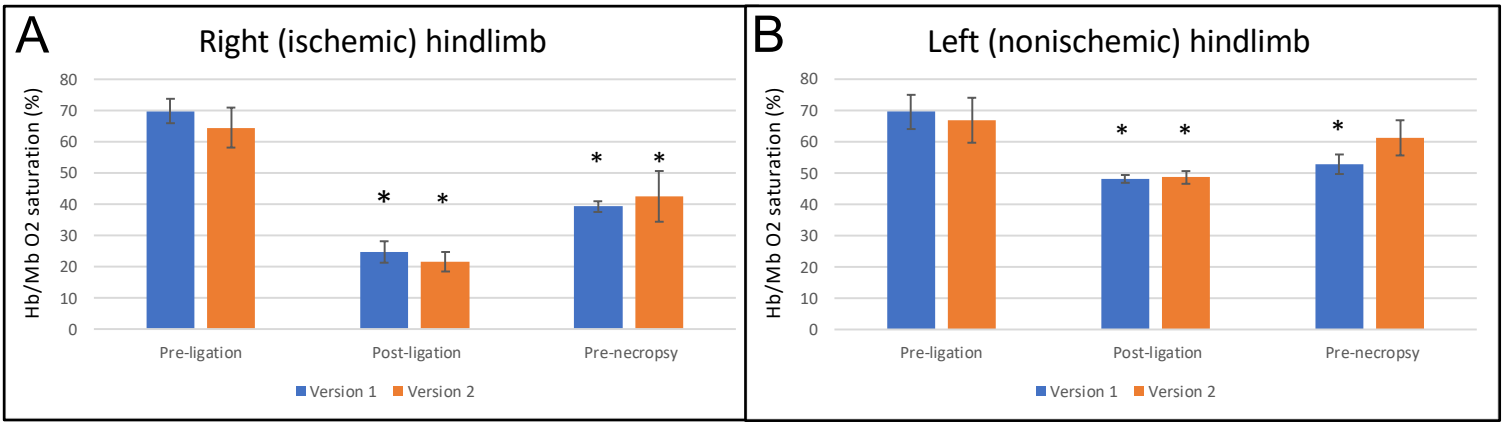

Fig tf07. Muscle hemoglobin/myoglobin oxygen saturation (Moxy), Version 1 *vs.* 2. (A & B) Right and left hindlimb, respectively. Each bar represents mean ± sd of all measurements from each subject at each time point; ≥2 measurements were taken at a constant location (medial thigh) at each time point. *$p < 0.05$ compared to Pre-ligation.

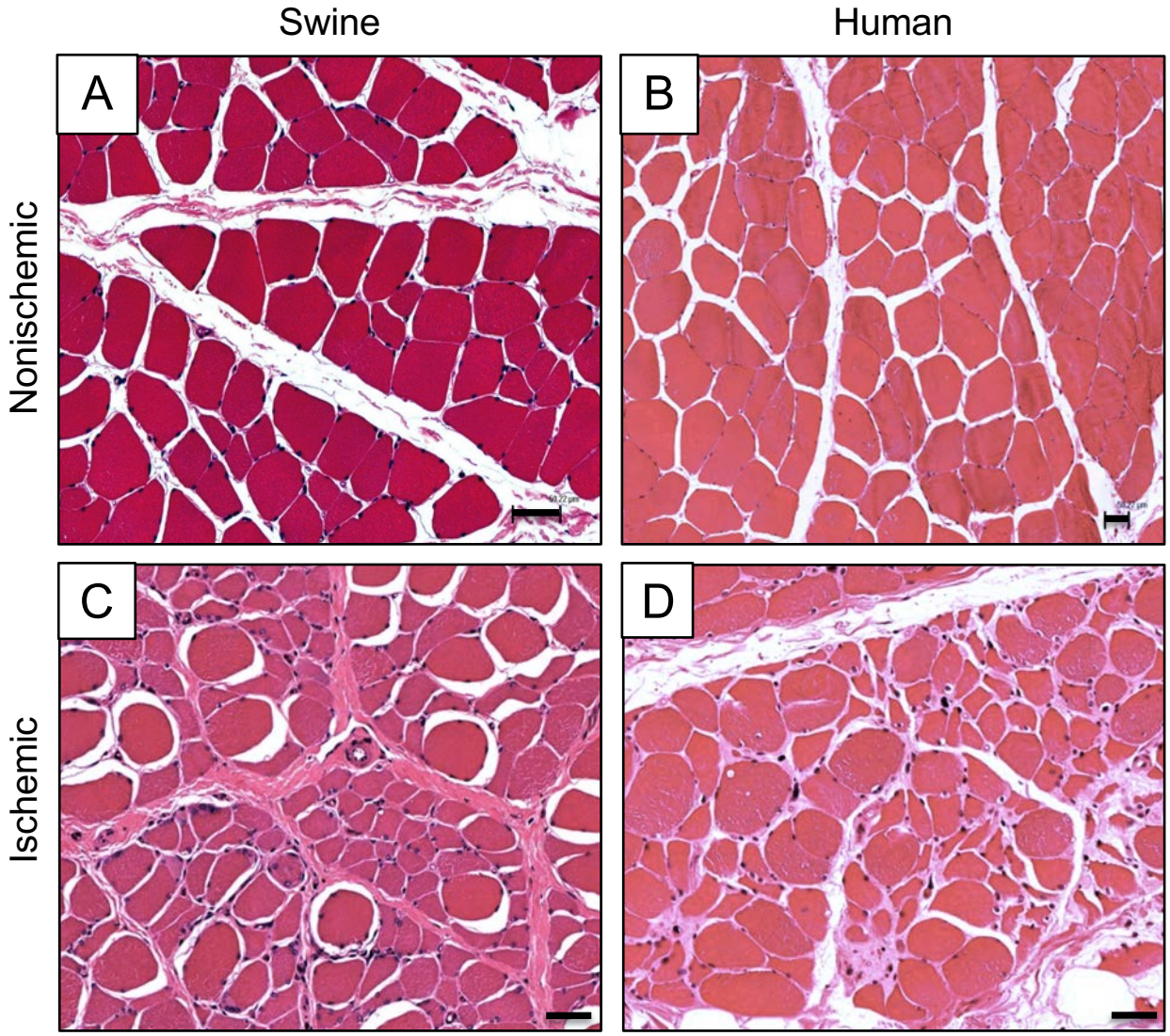

Fig tf08. Ischemic myopathy in porcine vs. human subjects. (A & B) Nonischemic muscle, human vs. porcine, respectively. **(C & D)** Ischemic muscle, human vs. porcine, respectively. Sample from both human and porcine subjects were taken from the gastrocnemius muscle. Clinical specimens derived from a separate research protocol that was previously published [insert reference]. Porcine tissue was from the present study (from pre-ligation and pre-necropsy biopsies). H&E; bars = 50 µm.

SUPPLEMENTAL FIGURES

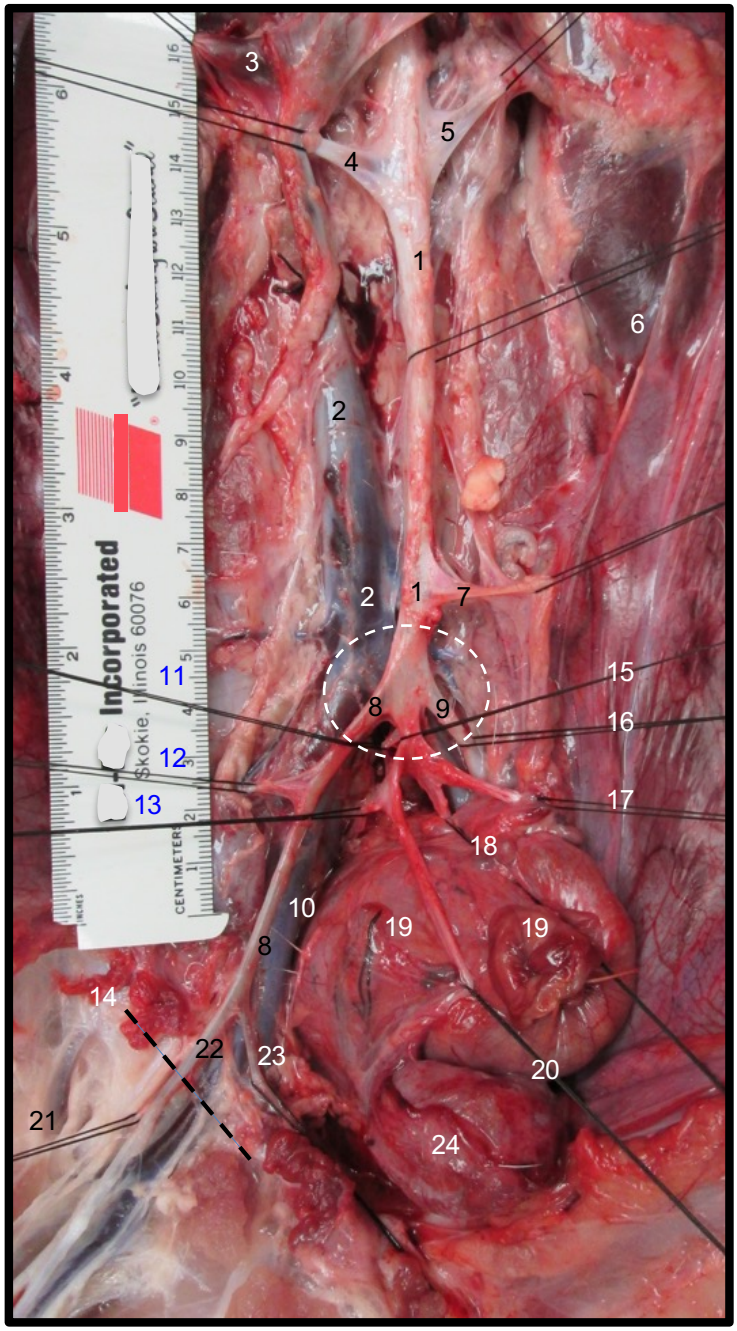

Fig tf09S. Relevant anatomy of the porcine hindlimb. Nonfixed postmortem dissection of the distal aorta, pelvis, and proximal right hindlimb in the pig. Dashed circle indicates aortic trifurcation.

1. Infrarenal aorta
2. Inferior vena cava
3. Right renal vein
4. Right renal artery
5. Left renal artery
6. Lower pole left kidney
7. Internal mesenteric artery (on silk loop)
8. Right external iliac artery
9. Left external iliac artery
10. Right external iliac vein
11. Middle sacral artery (on silk loop, posterior)
12. Right circumflex iliac artery (on silk loop)
13. Parietal branch of the right internal iliac artery on silk suture
14. Approximate level of inguinal ligament
15. Common internal iliac trunk (on silk loop)
16. Left external iliac artery (on silk loop)
17. Parietal branch of the right internal iliac artery on silk suture
18. Visceral branch of LIIA (on silk loop)
19. Rectal stump
20. Visceral branch of RIIA (on silk loop)
21. Right circumflex femoral artery (on silk loop)
22. Right superficial femoral artery
23. Right profunda femoral artery on silk suture
24. Urinary bladder

Fig. tf10S. Incision for retroperitoneal dissection. Anesthetized porcine subject is supine, with overhead view of ventral chest, abdomen, and pelvis; cephalad is toward top of image. Freshly closed incision indicated with arrows. Ruler is 15 cm long.

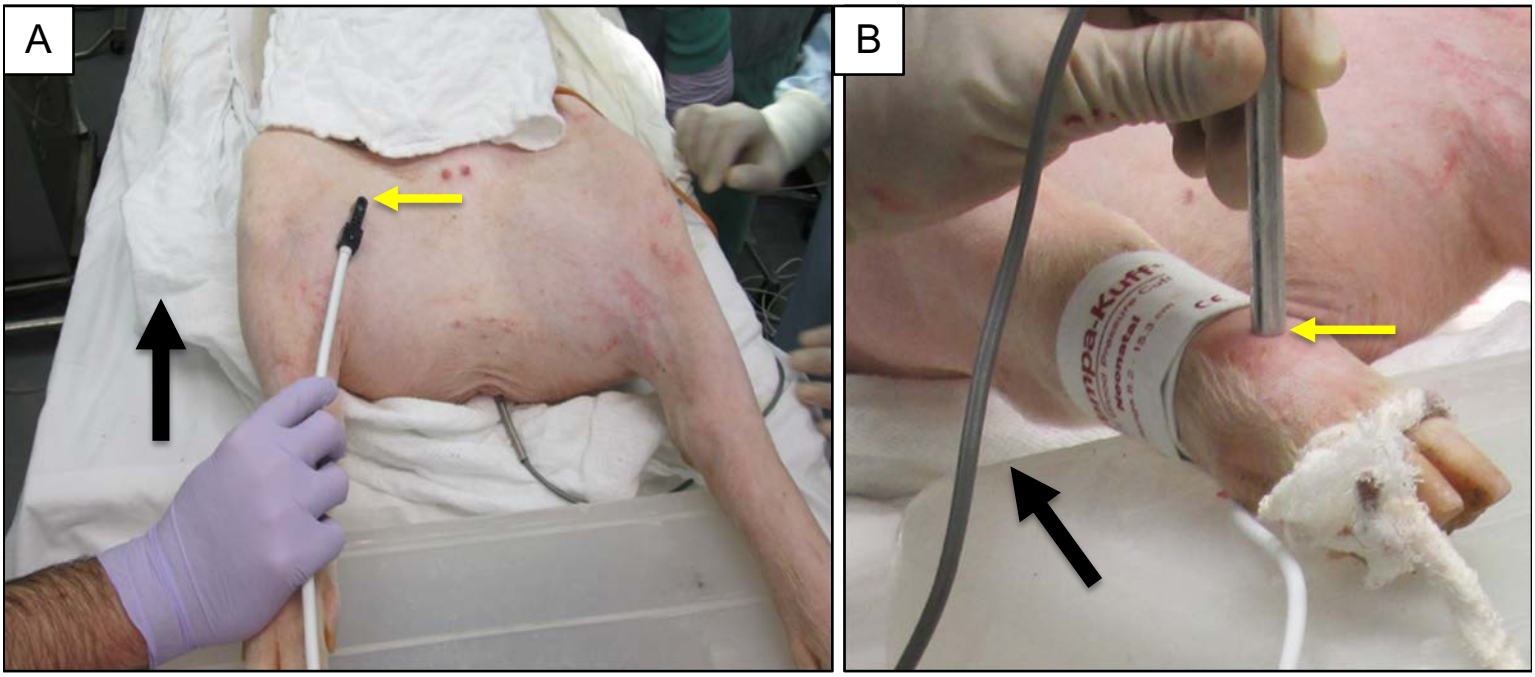

Fig tf11S. Measurements of Moxy and ABI in pigs. (A) Transcutaneous measurement of muscle hemoglobin/myoglobin oxygen saturation (Moxy). The Moxy instrument probe (arrow) has been placed over the right medial thigh of the subject. **(B)** Doppler of dorsalis pedis artery (yellow arrow) in the right distal hindlmb, for determination of arterial pressure index. Blood pressure cuff is visible just proximal to doppler probe. Black arrow = cephalad.

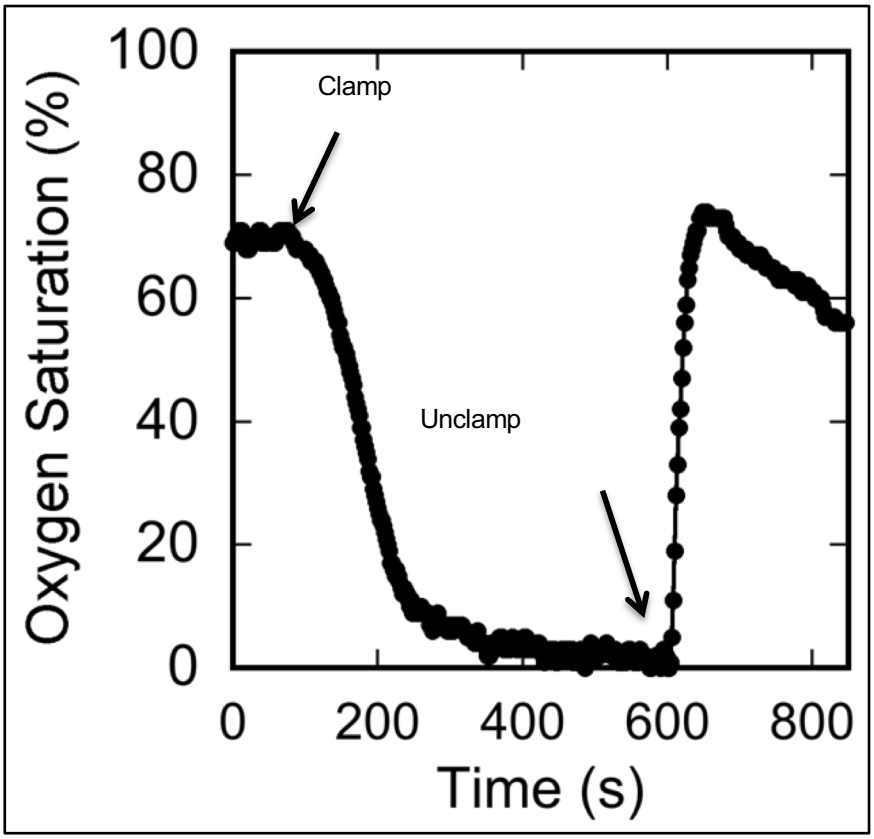

Fig tf12S. Sample tracing of muscle hemoglobin/myoglobin oxygen saturation (Moxy). The plot shows Moxy oximetry readings from of the porcine right medial thigh before, during, and after clamping of the right external iliac artery. There was an abrupt decrease in muscle oxygenation when the femoral artery was clamped and an abrupt increase in oxygenation when the artery was unclamped.

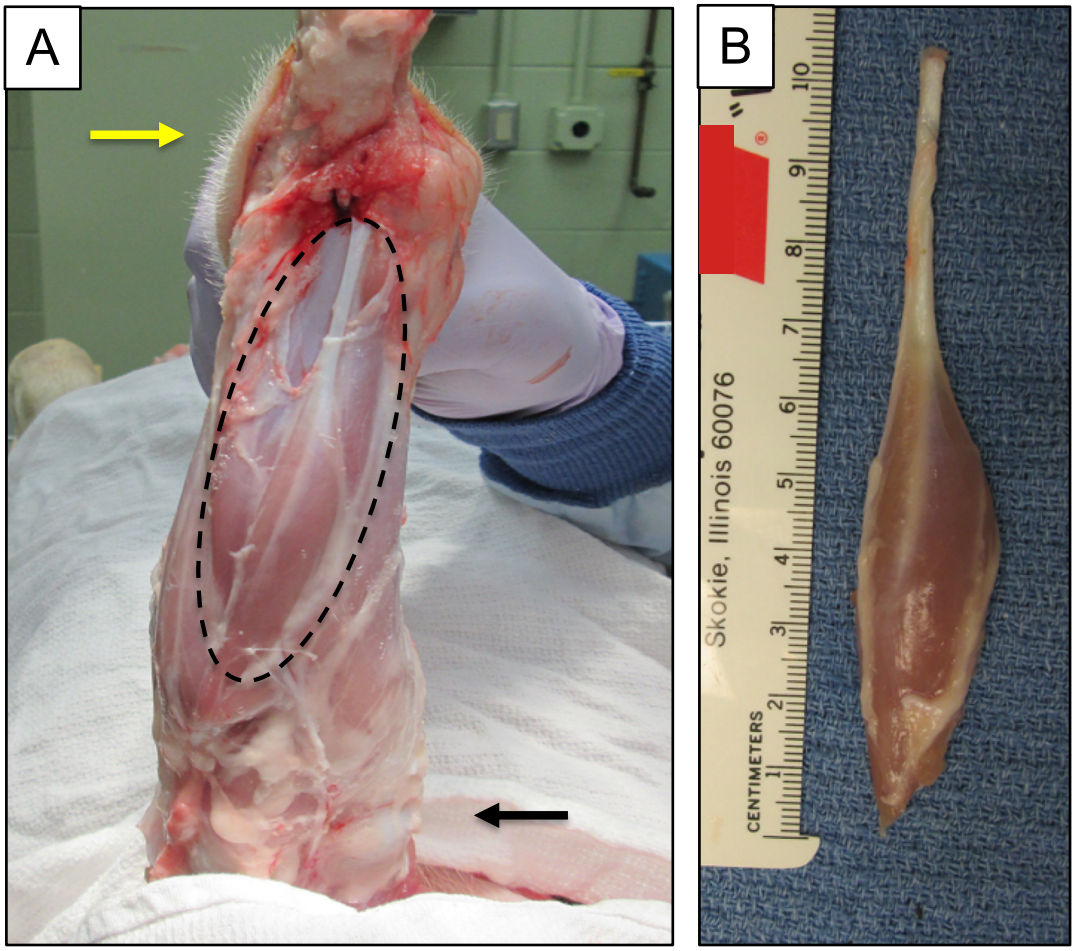

Fig tf13S. Postmortem dissection of porcine hindlimb. (A) Posterior view of right hindlimb, elevated; distal is at top of image, lateral is at left of image; yellow arrow indicates level of ankle joint; black arrow indicates level of knee joint. Gastrocnemius muscles have been dissected away, and are not visible. Dashed oval = plantaris muscle. **(B)** Explanted right plantaris muscle from panel A.